Carina Heisig[1,*]
Jelka Diedenhoven[1,2]
Christopher Jensen[3]
Helmut Gehrke[3]
Thomas Turek[1]

Selective Hydrogenation of Biomass-Derived Succinic Acid: Reaction Network and Kinetics

The conversion of bio-based succinic acid (SA) to the value-added chemicals 1,4-butanediol (BDO), γ-butyrolactone (GBL), and tetrahydrofuran (THF) can replace the corresponding petrochemical production routes to achieve a sustainable process. The reaction network for aqueous-phase catalytic hydrogenation of succinic acid over a supported Re-Pd catalyst was identified and the reaction kinetics was determined. With the developed kinetic model, the composition of the product mixture regarding the desired products (BDO, GBL, THF) can be described as a function of educt concentration, temperature, and pressure. The maximum BDO yield was achieved at high pressure and low temperature, while low pressure and high temperature favored GBL and THF production.

Keywords: Bimetallic catalyst, 1,4-Butanediol, Reaction kinetics, Selective hydrogenation, Succinic acid

Received: June 07, 2019; *revised:* October 28, 2019; *accepted:* December 17, 2019

DOI: 10.1002/ceat.201900324

Supporting Information available online

1 Introduction

Through the industrial revolution at the end of the 18th century, fossil fuels (coal, oil, and natural gas) were established as main resources. Nowadays, the majority of chemicals are produced from these resources, resulting in the consumption of more than 1 billion barrels of oil per year by the chemical industry [1]. A major problem related to the consumption of fossil fuels is the emission of huge amounts of carbon dioxide reaching 33.4 billion tons in 2017 [2]. onsidering the environmental impacts, alternative sustainable processes based on renewable resources such as sugars, sugar alcohols, oils, and lignocellulose become increasingly attractive.

1,4-Butanediol (BDO) is a high-added-value chemical and an important intermediate for many chemical processes. It is used in polymerization processes for the synthesis of polyesters, polyurethanes, and polyethers [3]. Moreover, it is the most relevant raw material to produce the chemical intermediates γ-butyrolactone (GBL) and tetrahydrofuran (THF). Those components are used in the chemical, pharmaceutical, and textile industry as well as in agriculture.

Since the 1950s, BDO, GBL, and THF are mostly produced via Reppe synthesis and integrated steps [4–6]. However, the handling of the starting materials formaldehyde and acetylene is difficult and the high energy demand is disadvantageous. Alternative production routes are based on the hydrogenation of maleic acid (MA) derivatives such as anhydrides, acids, and esters [7]. With regard to sustainable processes and new bio-derived building block chemicals, succinic acid (SA) has the ability to replace the current maleic anhydride platform. Thus, over the last decade, the production of SA from sugars by anaerobic fermentation has been the subject of intensive development. This resulted in R&D, pilot plants, and large-scale production realized by several companies (e.g., BioAmber, Reverdia, Myriant Technologies LCC) [8, 9].

After the fermentation process SA is obtained in aqueous phase [10, 11]. The product distribution of SA hydrogenation varies with the employed catalysts and operation conditions. Various heterogeneous catalysts have been described as highly efficient for the hydrogenation of SA or MA in aqueous phase. Besides monometallic catalysts containing noble metals, i.e., palladium, ruthenium, and rhenium, as active species [12–17] various bimetallic and trimetallic catalysts on different supports, i.e., activated carbon, TiO_2, Al_2O_3, SiO_2 or ZrO_2, are mentioned. Examples of these catalysts are Pd-Re/C [18, 19] or Pd-Re/TiO_2 [20, 21], Pd-Zr/C [22], Ru-Re/C [23–25], Ru-Sn/ZrO_2 [26], Pt-Re/C [27, 28], and Pd-Re-Ag/C [29].

However, little work has been done to predict the reaction conditions of aqueous-phase hydrogenation of SA required to produce an industrially relevant product composition [30].

[1]Carina Heisig, Dr.-Ing. Jelka Diedenhoven, Prof. Dr.-Ing. Thomas Turek
heisig@icvt.tu-clausthal.de
Clausthal University of Technology, Institute of Chemical and Electrochemical Process Engineering, Leibnizstrasse 17, 38678 Clausthal-Zellerfeld, Germany.

[2]Dr.-Ing. Jelka Diedenhoven
Covestro Deutschland AG, Kaiser-Wilhelm-Allee 60, 51373 Leverkusen, Germany.

[3]Dr. Christopher Jensen, Dr. Helmut Gehrke
thyssenkrupp Industrial Solutions AG, Neubeckumer Strasse 127, 59320 Ennigerloh, Germany.

Therefore, we focus in our study on the identification of the reaction network and the development of the reaction kinetics for aqueous-phase catalytic hydrogenation of SA over a supported Re-Pd catalyst and aim to determine the optimum reaction conditions to maximize the yield of the target products BDO, GBL, and THF. For this purpose, a new kinetic model for the hydrogenation of aqueous SA solution was developed that allows the quantitative description of the product composition as a function of educt concentration, temperature, and pressure.

2 Experimental

2.1 Materials

Succinic acid (≥ 99.0 wt %), 1,4-butanediol (≥ 99.0 wt %), γ-butyrolactone (≥ 99.0 wt %), and tetrahydrofuran (≥ 99.9 wt %) were received from Sigma-Aldrich. The water used for high-performance liquid chromatography (HPLC) calibrations was supplied by an ultrapure water device from Sartorius AG (Arium 611VF, 18.2 Ω cm, 0.055 µS cm^{-1} at 25 °C). Water used for hydrogenation experiments was prepared with a water demineralizer supplied by behr Labor-Technik (behropur® E28dK, 0.5 µS cm^{-1} at 25 °C). The catalyst (4 wt % Re-2 wt % Pd on activated carbon) was manufactured individually by Heraeus. It was supplied wet and did not undergo any pretreatment before usage. A particle diameter of x_{50} = 25 µm was measured with a particle size analyzer (Cilas, type 1180). Different batches of the catalyst (batch a (121560): loss on drying 55.0 wt %, batch b (140988): loss on drying 52.5 wt %) were used for the experiments.

2.2 Hydrogenation Experiments

The hydrogenation experiments were carried out in a laboratory plant supplied by Mothes Hochdrucktechnik GmbH (see Supporting Information Sect. S1). In addition to the stirred-tank reactor (stainless steel 1.4571, reactor volume 4 L, temperature up to 250 °C, pressure up to 200 bar), the plant consisted of gas supply and dosing, reactor periphery, sampling, and plant control. The double-jacketed vessel was temperature-controlled with a heating medium (Julabo HS 250) and a thermostat (Labortechnik Medingen, type TC250). The temperature of the reaction medium was measured by a resistor-type thermometer (Temperatur Messelemente Hettstedt GmbH, type Pt 100). A gassing stirrer, connected by magnetic coupling with the agitator (Parr Instrument GmbH, type 2164 HC and CAT M.Zipperer GmbH, type R100C), introduced the gas into the reaction medium. The pressure inside the vessel was controlled by a manometer and a digital pressure transducer (Mothes Hochdrucktechnik, pressure range: 0–250 bar and WIKA, type S-10). Helium and hydrogen were supplied by two mass flow controllers (Bronkhorst High-Tech E.V.: F-230M 0.25 Ln min^{-1} and F-231M: 5 Ln min^{-1}). Automated liquid sampling (HiTec Zang, type IL-Autosam 360) was done through an outlet in the reactor wall with a set of sintered metal frits (supelco, pore diameter 0.5–10 µm) hindering the catalyst from leaving the reactor.

In a typical run, catalyst powder and aqueous SA solution (range: 0.067–0.333 $g_{cat}g_{SA}^{-1}$) were introduced into the vessel and heated to the set temperature (range: 140–200 °C) under reduced stirring speed (250 rpm) whereby the hydrogen pressure was regulated to the desired value (range: 90–175 bar). The lower stirring speed guaranteed a homogeneous temperature distribution of the reaction solution without dispersing the catalyst particles. After the start-up process, a reactant conversion up to 10 % was typically observed. After reaching the specified temperature and pressure, the reaction was initiated by increasing the stirring speed to 1000 rpm to avoid mass transfer limitations. During the experiments the pressure was kept constant by re-dosing the hydrogen consumed by the hydrogenation reactions. For the determination of the reaction network and reaction kinetics of SA hydrogenation, experiments at different pressure, temperature, reactant concentration, and amount of catalyst were conducted.

The chemical equilibrium between the intermediates GBL and γ-hydroxybutyric acid (GHB) was also investigated using the same reactor as for SA hydrogenation. In a typical run, an aqueous solution of GBL was heated to the set temperature (range: 150–200 °C) at a stirring speed of 500 rpm while the pressure was kept constant at 175 bar to prevent evaporation of the aqueous solution. The pH value of the solution was adjusted to pH 6 using 37 wt % hydrochloric acid before being introduced into the reactor.

The samples with a mass of approx. 6 g (plus 10 g to clean the tubing) taken from the reactor were analyzed using an HPLC device equipped with a refractive index detector tempered at 30 °C (BioRad Aminex® HPX-87H at 25 °C, 4 mmol L^{-1} H_2SO_4 as mobile phase, flow rate of 0.7 mL min^{-1}, injection volume 20 µL). For better comparability of the temporal profiles of remaining educt concentration and yield in dependence on the catalyst amount m_{cat}[1)], the time t is replaced by a modified time t_{mod} (Eq. (1)).

$$t_{mod} = \frac{t m_{cat}}{V_{sol}} \tag{1}$$

Here, the volume of the reaction solution V_{sol} also takes into account the volume decrease by liquid sampling while the loss by water evaporation was negligibly small. On the other hand, the liquid phase concentrations of the volatile components were corrected by the evaporated amount of those species (see Supporting Information Sect. S4). The yield $Y_{p,e}$ is defined as the amount of product p formed during reaction related to the amount of educt e at the start of the reaction (Eq. (2)). Since organic components with variable carbon numbers are formed, the stoichiometry of the reactions is taken into account by the stoichiometric coefficients ν_i and the number of carbon atoms β_i. The mass balance during the hydrogenation experiments was assessed through the sum of the yields (Eq. (3)).

$$Y_{p,e} = \frac{c_p - c_{p,0}}{c_{e,0}} \frac{\nu_e}{\nu_p} \frac{\beta_p}{\beta_e} \tag{2}$$

$$\text{mass balance} = \sum Y_{p,e} \tag{3}$$

1) List of symbols at the end of the paper.

3 Determination of the Reaction Network

For the determination of the product spectrum during SA hydrogenation, a first experiment with an educt concentration of 0.423 $mol_{SA}L_{sol}^{-1}$ and a catalyst loading of 0.0067 $g_{cat}g_{sol}^{-1}$ was carried out at 180 °C and 175 bar. The resulting concentration profiles as a function of modified time are presented in Figs. 1a and 1b. It can be seen that SA was completely consumed after about 16 h (4.2×10^5 s $g_{cat}L_{sol}^{-1}$) under formation of BDO, GBL, and THF as main products while GHB, butyric acid, *n*-butanol, propionic acid, and *n*-propanol were observed as by-products. The mass balance was almost closed (>90 mol %) with the remaining amount most likely consisted of gaseous species (e.g., CO, CO_2, methane) and volatile components (e.g., THF, *n*-propanol, *n*-butanol) [29, 30].

These findings are in good agreement with previous publications [13, 18]. Minh et al. observed for the same type of catalyst (4 wt % Re–2 wt % Pd/C), similar reaction conditions (180 °C, 150 bar), a higher SA concentration (1.334 instead of 0.423 $mol_{SA}L_{sol}^{-1}$), and a higher catalyst amount (0.133 instead of 0.067 $g_{cat}g_{SA}^{-1}$) a BDO yield of 4 mol % at full SA conversion [18] which is in very good agreement with our own measurements corresponding to 43.4 mol % BDO.

The secondary products and intermediates BDO, GBL, and THF were also used as reactants (0.423 mol L_{sol}^{-1}, 0.0067 $g_{cat}g_{sol}^{-1}$) in a further series of measurements. As an example, the results of GBL hydrogenation are displayed in Figs. 2a and 2b. As expected, part of the GBL was converted to GHB already at the start of the reaction (initial pH 5). Afterwards, the concentrations of these two components decreased synchronously verifying the chemical equilibrium between GBL and GHB. As main products, large amounts of BDO together with THF as well as small amounts of *n*-propanol and *n*-butanol were formed. During hydrogenation of THF, small amounts of BDO (0.75 mol % yield after 44 h reaction time) and *n*-propanol were detected. Finally, BDO hydrogenation produced minor amounts of *n*-propanol, *n*-butanol, and THF (1.98 mol % yield after 44 h reaction time), while GBL could be hardly detected (see Supporting Information S4 (a), (b)).

Based on these findings, a reversible reaction between THF and BDO can be assumed, whereas the reaction of GBL to BDO appears to be irreversible. The latter observation could be due to the high pressures applied during the experiments, since an equilibrium reaction between GBL and BDO has been described for gas-phase reactions conducted at lower pressure [31]. Since the GBL hydrogenation quite obviously revealed an equilibrium reaction between GBL and GHB (Fig. 2a), this reaction (Eq. (4)) was studied in more detail. The equilibrium between GBL and GHB depends on reaction temperature and pH value of the solution [32], while a dependency on pressure is not expected for a liquid-phase reaction.

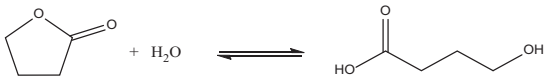

(4)

Due to the small concentrations of GBL (less than 1 mol L^{-1}) the amount of water in the reaction system is nearly constant. Thus, the law of mass action and the equilibrium constant K_{eq} can be simplified to Eq. (5) [32, 33].

$$K_{eq} = \frac{c_{GHB}}{c_{GBL}} \tag{5}$$

The chemical equilibrium is superimposed by the protolytic equilibrium of GHB. If GHB is dissociated to its anion, the free acid is no longer available for the reaction to GBL and the hydrolytic equilibrium is shifted to GHB [34]. Therefore, a higher pH value of the solution favors the conversion of GBL to GHB. At low pH values, GHB is present as a free acid in the

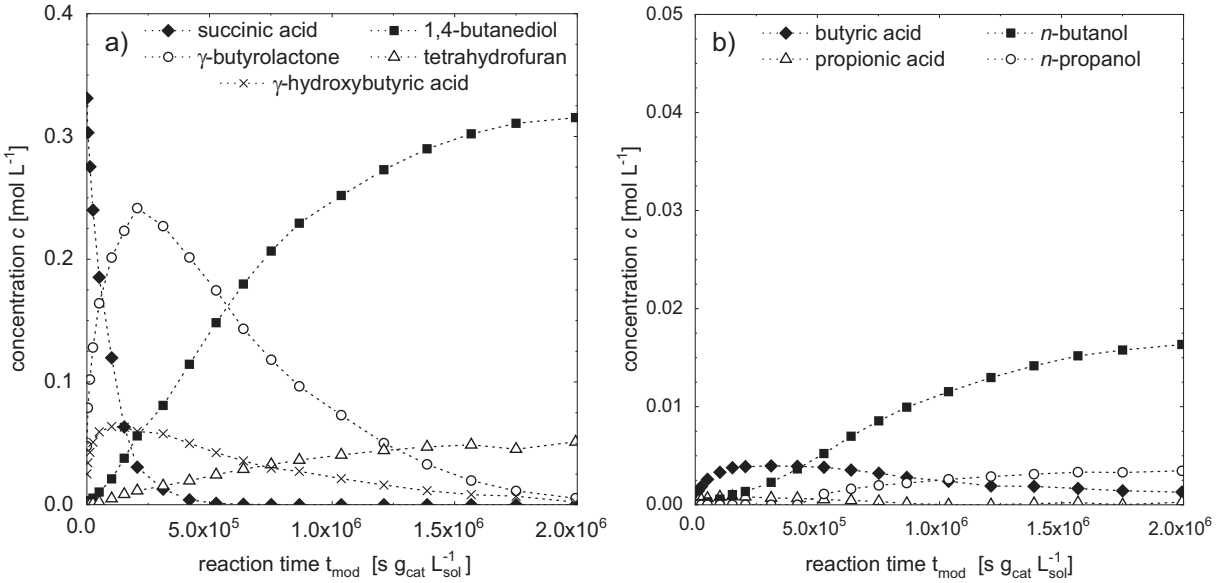

Figure 1. Concentration profiles during hydrogenation of aqueous SA solution. Catalyst batch b; reaction conditions: 180 °C, 175 bar, 0.423 $mol_{SA}L_{sol}^{-1}$, 0.0067 $g_{cat}g_{sol}^{-1}$. (a) Main products, (b) Side products.

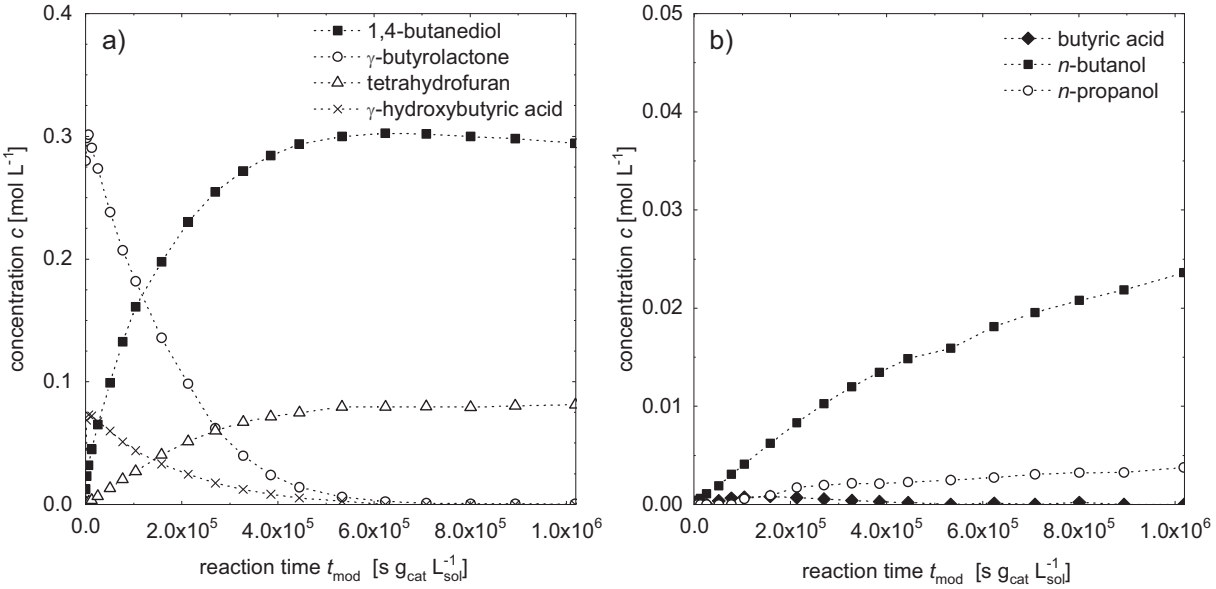

Figure 2. Concentration profiles during hydrogenation of aqueous GBL solution. Catalyst batch b; reaction conditions: 180 °C, 175 bar, 0.423 $mol_{GBL}L_{sol}^{-1}$, 0.0033 $g_{cat}g_{sol}^{-1}$. (a) Main products, (b) side products.

solution, whereby dissociation can be suppressed by a strong acid present (phosphoric or hydrochloric acid) to adjust the pH value. The temperature dependency on the equilibrium constant was described via the Van't Hoff equation (6).

$$\frac{\mathrm{d}\ln K_{eq}}{\mathrm{d}T} = \frac{\Delta_r H^0}{RT^2} \tag{6}$$

The standard enthalpy of reaction $\Delta_r H^0$ from literature and the value based on our measurements are summarized in Tab. 1. In agreement with Coffin et al. [33] , the hydrolysis of GBL to GHB appears to be a slightly exothermic reaction.

Table 1. Reaction enthalpies for the chemical equilibrium between GBL and GHB.

Source	pH value [–]		Temperature range [°C]	$\Delta_r H^0$ [kJ mol^{-1}]
	Beginning	Equilibrium		
[32, 33]	2		15–35	3.606 ± 0.62
[32, 33]	2		25–50	–2.956 ± 1.77
Measured value	6	3–4	150–200	–5.49 ± 0.35

Based on the hydrogenation experiments and the investigated equilibrium reactions the following reaction network is proposed (Fig. 3). First SA is converted to GBL, which is assumed to be in chemical equilibrium with GHB, and subsequently reacts to BDO, THF, and the secondary components butyric acid, *n*-butanol and *n*-propanol. In contrast to GBL hydrogenation, propionic acid was detected when SA was hydrogenated. Thus, a direct conversion of SA to propionic acid is assumed. The observed decrease of the propionic acid concentration suggests a secondary reaction to *n*-propanol. Since SA, THF, and BDO lose one C atom during conversion to propionic acid and *n*-propanol, the formation of gaseous products is a logical consequence [18, 29].

4 Determination of Reaction Kinetics

Since the hydrogenation reactions take place at the catalyst surface in liquid phase, hydrogen solubility data are required. In order to determine the intrinsic kinetics, the absence of external and internal mass transport influences must be ensured. Subsequently the parameters of the reaction rate equations, i.e., rate constants, reaction orders, and inhibition terms, are determined by adapting the simulated results to the experimentally derived concentration profiles.

4.1 Determination of the Hydrogen Solubility

Due to lack of data on the solubility of hydrogen in aqueous succinic acid solutions, solubility data of hydrogen in water were calculated according to Schäfer [30] (see the Supporting Information Sect. S2). This simplification is justified as the reaction solution consists of up to 95 wt % water and it has been shown that the influence of small amounts of organic components on hydrogen solubility is negligible [27]. The hydrogen concentrations for the relevant reaction conditions are summarized in Tab. 2.

4.2 Evaluation of Mass Transport Limitations

The possible influence of mass transport limitations was determined with standard Sherwood correlations for the external mass transfer and a simplified Thiele modulus approach for

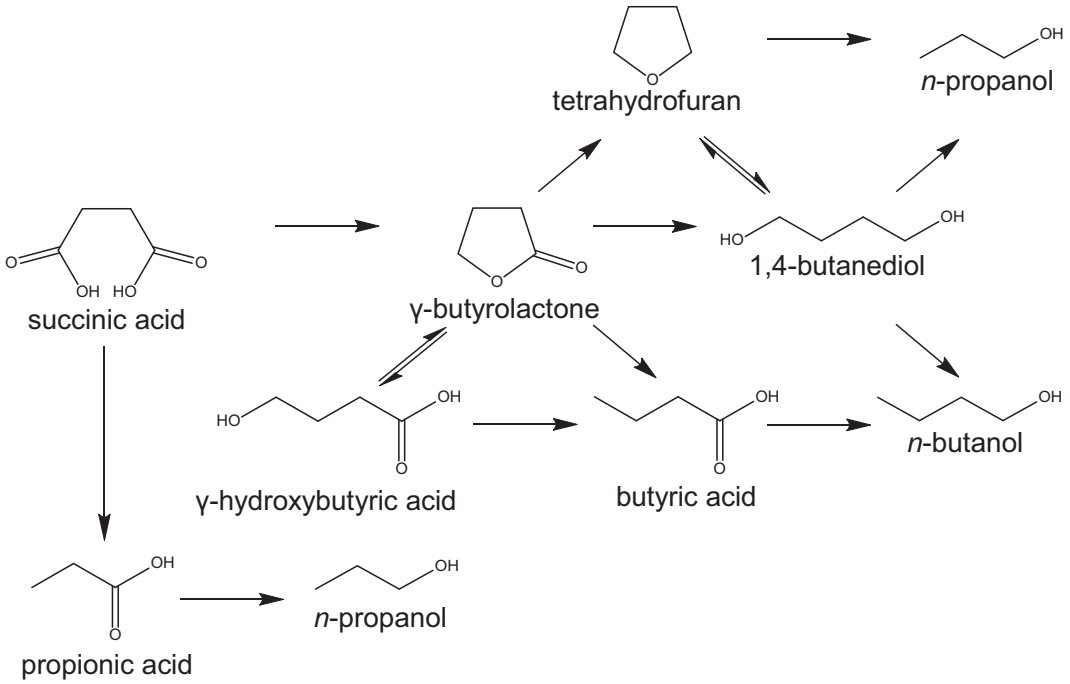

Figure 3. Reaction network for the hydrogenation of SA.

Table 2. Solubility of hydrogen in mol L^{-1} for the reaction conditions of SA hydrogenation.

Pressure p [bar]	Temperature T [°C]			
	140	160	180	200
90	0.071	0.087	0.104	0.118
125	0.100	0.124	0.149	0.173
150	0.120	0.150	0.182	0.213
175	0.141	0.176	0.214	0.252

the internal mass transfer (see Supporting Information Sect. S3). For all hydrogenation experiments performed, the influence of the mass transport was dominated by the gas-liquid mass transfer. However, even in the worst case (c_0 = 0.423 $mol_{SA}L_{sol}^{-1}$, 0.0067 $g_{cat}g_{sol}^{-1}$, 200 °C, 90 bar) the corresponding overall catalyst efficiency was still larger than 0.99. Thus, all measured data could be used for the estimation of the intrinsic reaction kinetics.

4.3 Estimation of the Kinetic Parameters

The liquid-phase reactant concentrations were corrected taking the gas-liquid equilibria for the volatile species THF, *n*-butanol, and *n*-propanol into account (see Supporting Information Sect. S4). The evaporation of water was neglected, since the water content in the gas phase was well below 1 mol % in all cases. For estimation of the kinetic parameters, the complete reaction network (Fig. 3) was simplified as illustrated in Fig. 4. Here, the minor components with low yields (butyric acid and propionic acid with < 1 mol %, *n*-butanol and *n*-propanol with < 5 mol %) were not taken into account.

Given the equilibrium between GBL and GHB, these components were combined to a pseudo component while the fraction of GHB in the pseudo component was calculated with the equilibrium constant K_{eq}. Moreover, the reaction between THF and BDO was neglected while a consecutive reaction of BDO to side components was assumed (see Fig. 4, reaction 4). With this reaction, the decrease of the mass balance by formation of not measured gaseous species was also considered. For the worst case investigated (200 °C, 175 bar, 0.423 $mol_{SA}L_{sol}^{-1}$, 0.0067 $g_{cat}g_{sol}^{-1}$) the mass balance decreased by 8.9 mol % at full SA conversion and by 11.0 mol % at the end of the experiment. On average, the mass balance deficit amounted to approximately 3.9 mol % at full SA conversion and to about 5.8 mol % at the end of the experiments.

The kinetic parameters were estimated using gPROMS® (version 4.1.0) with the logarithmic likelihood function as objective function. For the reaction of SA to GBL as well as for the conversion of GBL to THF and the conversion of BDO to side components, simple power-law equations were used. The kinetics of the GBL to BDO reaction was described by a hyperbolic Eley-Rideal type equation. The temperature dependency of the equilibrium constant K_{eq} was calculated according to the Van't Hoff equation while activation energies according to the Arrhenius approach were used for the reaction rate constants.

The obtained kinetic parameters are summarized in Tab. 3. It has to be noted that different batches (a and b) of the same catalyst were used to carry out the hydrogenation experiments. While the kinetic parameters are largely identical for the two batches, the values for the activation energies differ slightly (values for batch b in brackets). However, these values are in the same order of magnitude as activation energies determined

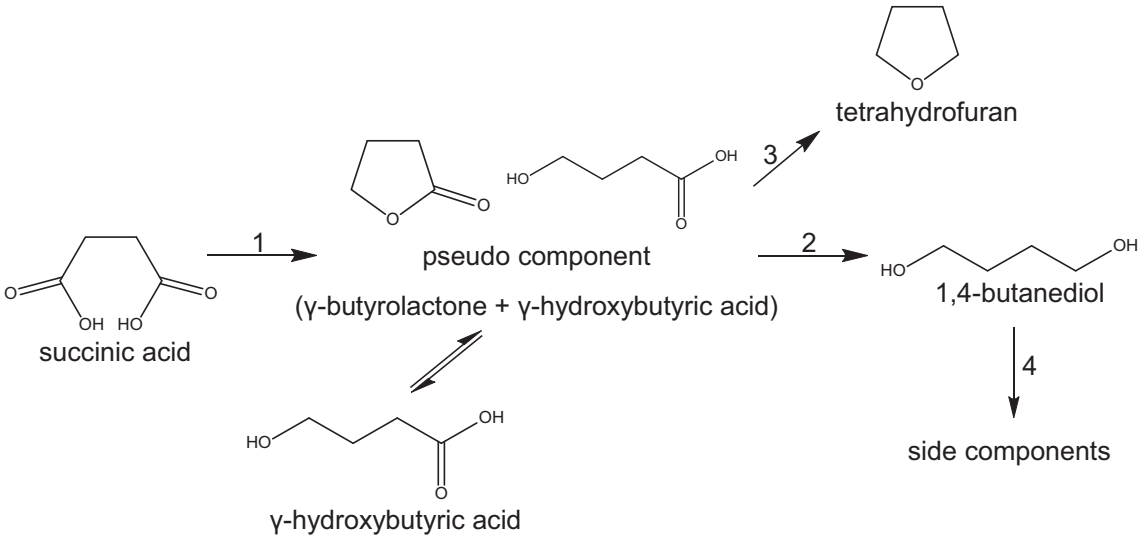

Figure 4. Reduced reaction network for the hydrogenation of SA.

by Di et al. at a similar catalyst (2.5 wt %Re–1.5 wt %Ru on activated carbon) [25]. It can be seen that the reaction enthalpy describing the hydrolysis of GBL to GHB (–8.04 kJ mol^{-1}) deviates slightly from the value resulting from the equilibrium measurements (–5.49 kJ mol^{-1}). This is most probably due to the complexity of the reaction mixture as there are numerous other species present in addition to GBL and GHB. The formed acids cause a slight decrease of the pH value resulting in a reduction of the equilibrium constant, which is in line with the dependency of the hydrolytic equilibrium on the pH value [34].

Table 3. Rate equations and kinetic parameters for the hydrogenation of aqueous SA solutions.

Equation	Parameter	Value[a)]
$r_1 = k_{0,1}\exp\left(-\frac{E_{a,1}}{R\cdot T}\right) c_{SA}^{n_{SA}} c_{H_2}^{m_{H_2,1}}$	$k_{0,1}$	12 $L_{sol}^{(n_i+m_{H_2,j})} s^{-1} g_{cat}^{-1} mol^{(1-n_i-m_{H_2,j})}$
	$E_{a,1}$	50710 J mol^{-1} (50320)
	n_{SA}	1
	$m_{H2,1}$	0.3
$r_2 = k_{0,2}\exp\left(-\frac{E_{a,2}}{RT}\right) \frac{K_{GBL}c_{GBL}}{(1+K_{GBL}c_{GBL})} c_{H_2}^{m_{H_2,2}}$	$k_{0,2}$	0.0012 $L_{sol}^{(n_i+m_{H_2,j})} s^{-1} g_{cat}^{-1} mol^{(1-n_i-m_{H_2,j})}$
	$E_{a,2}$	22030 J mol^{-1} (19980 J mol^{-1})
	K_{GBL}	2
	$m_{H2,2}$	1.2
$r_3 = k_{0,3}\exp\left(-\frac{E_{a,3}}{R\cdot T}\right) c_{GBL}^{n_{GBL}} c_{H_2}^{m_{H_2,3}}$	$k_{0,3}$	99840 $L_{sol}^{(n_i+m_{H_2,j})} s^{-1} g_{cat}^{-1} mol^{(1-n_i-m_{H_2,j})}$
	$E_{a,3}$	99870 J mol^{-1} (100820 J mol^{-1})
	n_{GBL}	0.8
	$m_{H2,3}$	0.4
$r_4 = k_{0,4}\exp\left(-\frac{E_{a,4}}{R\cdot T}\right) c_{BDO}^{n_{BDO}} c_{H_2}^{m_{H_2,4}}$	$k_{0,4}$	0.0012 $L_{sol}^{(n_i+m_{H_2,j})} s^{-1} g_{cat}^{-1} mol^{(1-n_i-m_{H_2,j})}$
	$E_{a,4}$	17500 J mol^{-1} (22390 J mol^{-1})
	n_{BDO}	2
	$m_{H2,4}$	1.5
$K_{eq} = K_{eq}^{\infty}\exp\left(-\frac{\Delta_r H}{RT}\right)$	$\Delta_r H$	–8040 J mol^{-1}
	K^{∞}_{eq}	0.026

[a)] Activation energies obtained with catalyst batch b are given in brackets.

The resulting fit for the temperature dependency of SA hydrogenation at 175 bar is exemplarily depicted in Figs. 5a–d. It can be seen that the simplified kinetic model allows a good description of the measured concentration profiles. Especially the main species SA, BDO, and THF can be described with a deviation of less than 10 % from the measured values. Only at low reactant concentrations (<0.2 mol L^{-1}) the deviations become larger. This may be caused by the definition of the pseudo compound, which does not distinguish between the individual reaction paths to a specific secondary product.

The comparison between measured and calculated values for the pressure dependence (see Supporting Information Figs. S5 (a)–(d)) and the influence of the educt concentration (see Supporting Information Figs. S6 (a)–(d)) also reveals that the kinetic model provides a description with good accuracy. Finally, the sum of the yields of all main products (BDO, THF, GBL including GHB), which are of equally high economic interest, are shown as a function of the modified time in Fig. 6a. It becomes

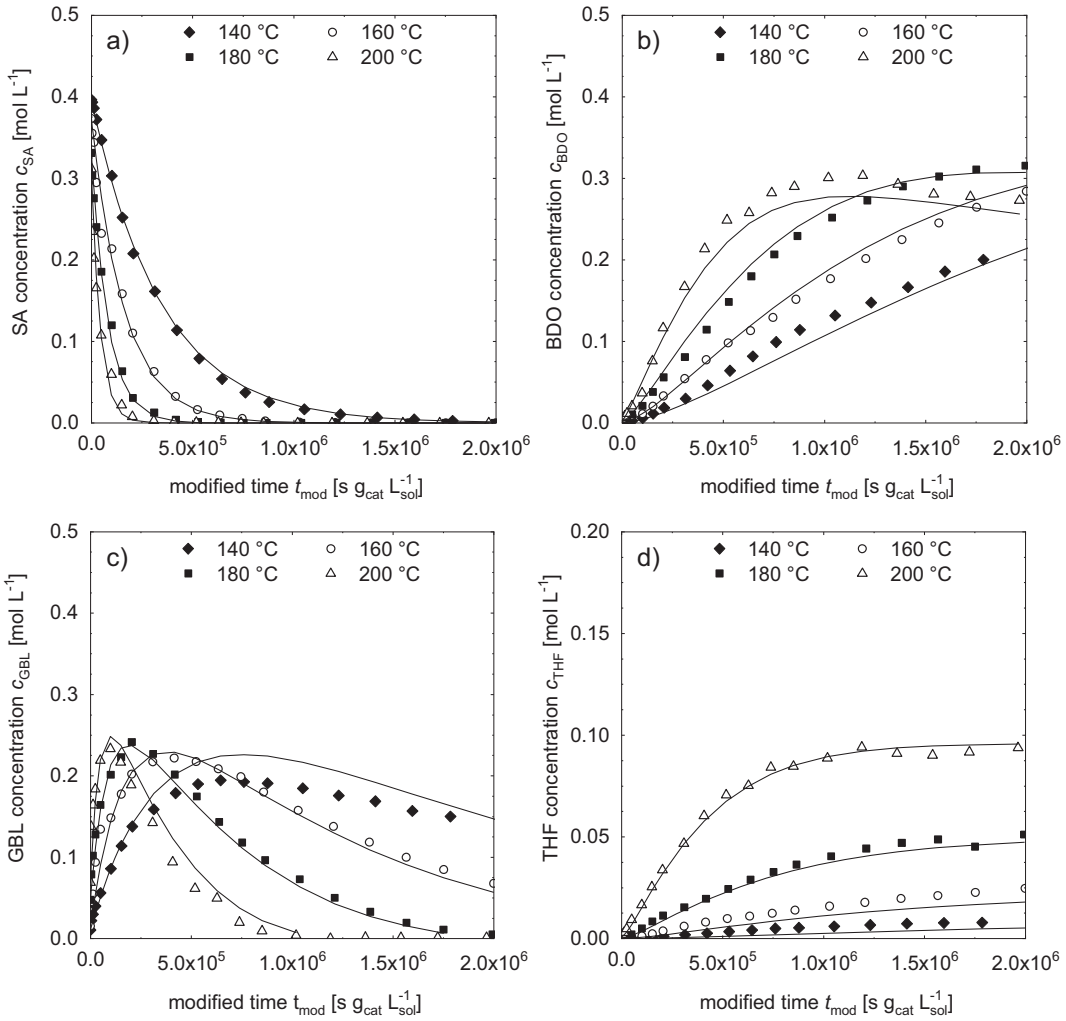

Figure 5. Measured (symbols) and calculated (lines) concentrations as a function of modified time and temperature during SA hydrogenation. Catalyst batch b, 175 bar, 0.423 $mol_{SA}L_{sol}^{-1}$, 0.0067 $g_{cat}g_{sol}^{-1}$).

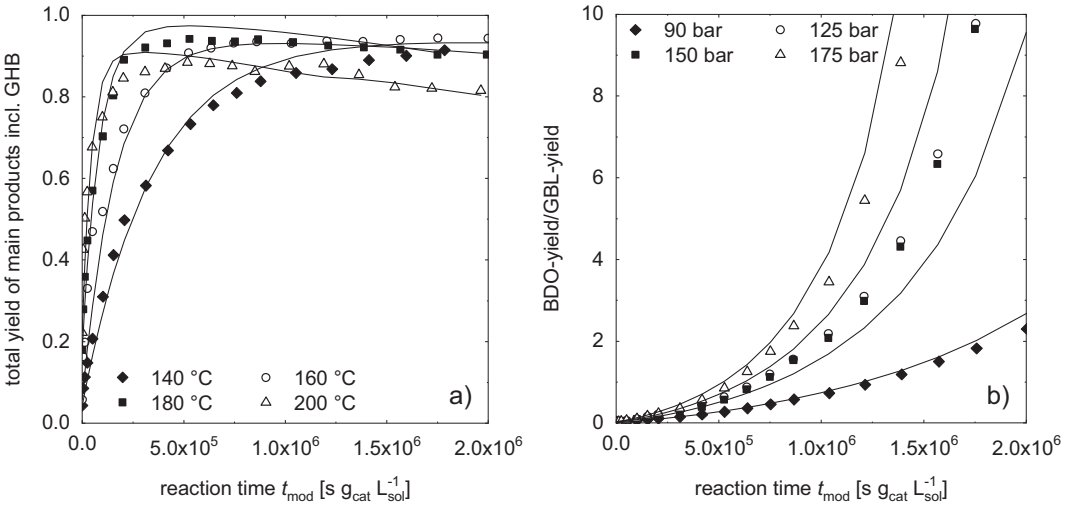

Figure 6. Measured (symbols) and calculated (lines) data of (a) total yield of main products (BDO, GBL, THF, GHB) for various temperatures at 175 bar and (b) pressure dependency of the ratio between BDO and GBL yields at 180 °C (catalyst batch b, 0.423 $mol_{SA}L_{sol}^{-1}$, 0.0067 $g_{cat}g_{sol}^{-1}$).

obvious that an operating temperature of 180 °C is optimal for achieving the highest amounts of main products with total yields exceeding 90 mol %. At higher temperatures, the degradation reaction of BDO is favored. In contrast, the variation of the operating pressure has no significant influence on the total yield of the valuable products.

However, the ratio between the main target products BDO and GBL can be strongly influenced by the reactor pressure (Fig. 6b). The highest ratio between BDO and GBL yields is achieved for long reaction times where the production of BDO is additionally favored by rising pressure. Thus, the process is very flexible and allows producing different ratios of GBL and BDO dependent on the current market situation.

5 Conclusion

The hydrogenation of aqueous succinic acid (SA) solutions yielding the main products 1,4-butanediol (BDO), γ-butyrolactone (GBL), and tetrahydrofuran (THF) was investigated by measurements in a stirred-tank batch reactor. In agreement with literature data it was found that a bimetallic 4 wt % Re–2 wt % Pd/activated carbon catalyst shows high selectivities towards these value-added products with total yields exceeding 90 mol % under optimum reaction conditions.

Based on systematic measurements with SA and intermediate products, a reaction network for SA hydrogenation consisting of 12 reactions including the main components BDO, GBL, THF, and GHB as well as the side components *n*-butanol, butyric acid, propionic acid, and *n*-propanol was developed. For evaluation of the subsequent systematic kinetic measurements as a function of temperature, pressure, and SA concentration, the reaction network was simplified.

Through assessment of mass transport limitations it was ensured that the intrinsic kinetics was measured in all cases. With the aid of suitable kinetic expression, the influence of the most important reaction conditions on the measured concentration profiles could be described with good accuracy. With this quantitative description of the reaction network, an optimum reaction temperature of 180 °C could be determined.

While the reactor pressure has little effect on the total yield of the main target products, the ratio between BDO and GBL can be enhanced at increasing pressure. In the next step, the determined reaction kinetics can be used to design suitable reactors for industrial production of bio-derived BDO, GBL, and THF.

Acknowledgment

The authors gratefully acknowledge the financial support provided by thyssenkrupp Industrial Solutions AG and thank for the beneficial discussions with our project partners.

The authors have declared no conflict of interest.

Symbols used

c	[mol L^{-1}]	concentration
E_a	[J mol^{-1}]	activation energy
$\Delta_r H$	[J mol^{-1}]	reaction enthalpy
$\Delta_r H^0$	[J mol^{-1}]	standard reaction enthalpy
k	$[L_{sol}^{\left(n_i+m_{H_2,j}\right)} s^{-1} g_{cat}^{-1} mol^{\left(1-n_i-m_{H_2,j}\right)}]$	reaction rate constant
k_0	$[L_{sol}^{\left(n_i+m_{H_2,j}\right)} s^{-1} g_{cat}^{-1} mol^{\left(1-n_i-m_{H_2,j}\right)}]$	frequency factor
K_{eq}	[–]	rate constant for Eley-Rideal mechanism
K_i	[–]	equilibrium constant
m	[g]	mass
$m_{H2,j}$	[–]	reaction order with respect to concentration of hydrogen in reaction j
n_i	[–]	reaction order with respect to concentration of component i
p	[bar]	pressure
R	[J $mol^{-1} K^{-1}$]	universal gas constant
r_j	[mol $s^{-1} g_{cat}^{-1}$]	rate of reaction j
t	[s]	time
t_{mod}	[s $g_{cat} L_{sol}^{-1}$]	modified time
T	[K]	temperature
V	[L]	volume
x_{50}	[µm]	mass-median radius
Y_i	[mol mol^{-1}]	yield of component i

Greek letters

ν	[–]	stoichiometric coefficient
β	[–]	number of carbon atoms

Sub- and superscripts

0	value for normal temperature and pressure at the start of the reaction
∞	value for infinite dilution
cat	catalyst
e	educt
eq	equilibrium
H_2	hydrogen
mod	modified
p	product
r	reaction
sol	solution

Abbreviations

BDO	1,4-butanediol
GBL	γ-butyrolactone
GHB	γ-hydroxybutyric acid
HPLC	high-performance liquid chromatography
MA	maleic acid
R&D	research & development
SA	succinic acid
THF	tetrahydrofuran

References

[1] M. Paster, J. L. Pellegrino, T. M. Carole, *Prospects for a Bio-based Industry*, Report, US Department of Energy, Washington, DC **2003**.

[2] BP p.l.c., *Statistical Review of World Energy* **2017**, www.bp.com/en/global/corporate/energy-economics/statistical-review-of-world-energy.html (Accessed on April 04, 2019)

[3] T. Kälin, S. Davis, K. Fujita, *CEH Marketing Research Report: 1,4-Butandiol* **2007**.

[4] W. Reppe, E. Keyssner, *DE 725326*, **1942**.

[5] W. Reppe, *Chem. Ing. Tech.* **1950**, *22 (17)*, 361–388. DOI: https://doi.org/10.1002/cite.330221302

[6] W. D. Reppe, W. D. Schmidt, A. D. Schulz, H. D. Wenderlein, *DE 890944*, **1953**.

[7] K. Lohbeck, H. Haferkorn, W. Fuhrmann, N. Fedtke, in *Ullmann's Encyclopedia of Industrial Chemistry*, Wiley-VCH, John Wiley & Sons, Vol. 22, Wiley-VCH, Weinheim **2000**, 145–155.

[8] S. Vaswani, *Bio-based succinic acid*, PEP Review, SRI Consulting, Menlo Park, CA **2010**.

[9] S. Bell, *Bio-based succinic acid*, Process Economics Program, IHS Chemical **2014**.

[10] P. Claus, H. Vogel, *Chem. Eng. Technol.* **2008**, *31 (5)*, 678–699. DOI: https://doi.org/10.1002/ceat.200700417

[11] C. Delhomme, D. Weuster-Botz, F. E. Kühn, *Green Chem.* **2009**, *11 (1)*, 13–26. DOI: https://doi.org/10.1039/B810684C

[12] S.-H. Chung, Y.-M. Park, M.-S. Kim, K.-Y. Lee, *Catal. Today* **2012**, *185 (1)*, 205–210. DOI: https://doi.org/10.1016/j.cattod.2011.08.011

[13] L. Corbel-Demailly, B.-K. Ly, D.-P. Minh, B. Tapin, C. Especel, F. Epron, A. Cabiac, E. Guillon, M. Besson, C. Pinel, *ChemSusChem* **2013**, *6 (12)*, 2388–2395. DOI: https://doi.org/10.1002/cssc.201300608

[14] R. Luque, J. H. Clark, K. Yoshida, P. L. Gai, *Chem. Commun.* **2009**, *35*, 5305–5307. DOI: https://doi.org/10.1039/B911877B

[15] B. Tapin, F. Epron, C. Especel, B.-K. Ly, C. Pinel, M. Besson, *ACS Catal.* **2013**, *3 (10)*, 2327–2335. DOI: https://doi.org/10.1021/cs400534x

[16] P. D. Vaidya, V. V. Mahajani, *J. Chem. Technol. Biotechnol.* **2003**, *78 (5)*, 504–511. DOI: https://doi.org/10.1002/jctb.816

[17] X. Di, Z. Shao, C. Li, W. Li, C. Liang, *Catal. Sci. Technol.* **2015**, *5 (4)*, 2441–2448. DOI: https://doi.org/10.1039/C5CY00004A

[18] D. P. Minh, M. Besson, C. Pinel, P. Fuertes, C. Petitjean, *Top. Catal.* **2010**, *53 (15–18)*, 1270–1273. DOI: https://doi.org/10.1007/s11244-010-9580-y

[19] Z. Shao, C. Li, X. Di, Z. Xiao, C. Liang, *Ind. Eng. Chem. Res.* **2014**, *53 (23)*, 9638–9645. DOI: https://doi.org/10.1021/ie5006405

[20] B.-K. Ly, D. P. Minh, C. Pinel, M. Besson, B. Tapin, F. Epron, C. Especel, *Top. Catal.* **2012**, *55 (7–10)*, 466–473. DOI: https://doi.org/10.1007/s11244-012-9813-3

[21] B. Tapin, F. Epron, C. Especel, B. K. Ly, C. Pinel, M. Besson, *Catal. Today* **2014**, *235*, 127–133. DOI: https://doi.org/10.1016/j.cattod.2014.02.018

[22] T. Werpy, J. G. Frye, Y. Wang, A. H. Zacher, *US 6670300*, **2001**.

[23] R. V. Chaudhari, C. V. Rode, R. M. Deshpande, R. Jaganathan, T. M. Leib, P. L. Mills, *Chem. Eng. Sci.* **2003**, *58 (3–6)*, 627–632. DOI: https://doi.org/10.1016/S0009-2509(02)00588-2

[24] N. N. Thakar, R. Jaganathan, R. V. Chaudhari, *AIChE J.* **2003**, *49 (12)*, 3199–3211. DOI: https://doi.org/10.1002/aic.690491219

[25] X. Di, C. Li, B. Zhang, J. Qi, W. Li, D. Su, C. Liang, *Ind. Eng. Chem. Res.* **2017**, *56 (16)*, 4672–4683. DOI: https://doi.org/10.1021/acs.iecr.6b04875

[26] P. A. Tooley, J. R. Black, *US 5985789*, **1997**.

[27] R.-H. Fischer, R. Pinkos, S. A. Schunk, J. Wulff-Döring, F. Stein, T. Nöbel, S. Huber, *US 7172989 B2*, **2005**.

[28] X. Di, C. Li, G. Lafaye, C. Especel, F. Epron, C. Liang, *Catal. Sci. Technol.* **2017**, *7 (22)*, 5212–5223. DOI: https://doi.org/10.1039/C7CY01039G

[29] J. R. Budge, T. G. Attig, S. E. Pedersen, *US 5473086*, **1995**.

[30] H. Schäfer, *Dissertation*, Universität Erlangen-Nürnberg, Erlangen **2005**.

[31] J. H. Schlander, T. Turek, *Ind. Eng. Chem. Res.* **1999**, *38*, 1264–1270. DOI: https://doi.org/10.1021/ie980606k

[32] M. T. Pérez-Prior, J. A. Manso, M. D. Garcia-Santos, E. Calle, J. Casado, *J. Org. Chem.* **2005**, *70*, 420–426. DOI: https://doi.org/10.1021/jo040271i

[33] F. D. Coffin, F. A. Long, *J. Am. Chem. Soc.* **1952**, *74*, 5767–5768. DOI: https://doi.org/10.1021/ja01142a507

[34] L. A. Ciolino, M. Z. Mesmer, R. D. Satzger, A. C. Machal, H. A. McCauley, A. S. Mohrhaus, *J. Forensic Sci.* **2001**, *46 (6)*, 1315–1323. DOI: https://doi.org/10.1520/JFS15152J

